

ASYNCHRONOUS AND TIME-DELAYED SENSOR FUSION OF A LASER SCANNER NAVIGATION SYSTEM AND ODOMETRY

Mariolino De Cecco¹, Luca Baglivo², Enrico Ervas², Enrico Marcuzzi²

¹ DIMS University of Trento, Italy, mariolino.dececco@ing.unitn.it

² CISAS University of Padova, Padova, Italy

Abstract: This paper presents a description of the ‘sensor fusion’ algorithm for our proprietary new navigation system, the LS_NAV, which is based on laser range scanning data inside natural environment. The fusion is exploited between odometric navigation and the LS_NAV. In the proposed algorithm the accuracy of both navigation systems is estimated as a function of the actual manoeuvre being carried out. The method allows compensating the drift of the incremental system estimation, high data rate and noise reduction of the LS_NAV estimates. Experimental verification is carried out using an autonomous vehicle.

Keywords: sensor fusion, AGV navigation, laser scanner.

1. INTRODUCTION

Autonomous Guided Vehicles are widely used in a huge number of fields such as factories, ports, hospitals, farms, etc., yet measuring a vehicle’s attitude and position (the pose) is still a challenging problem.

The measurement systems currently used can be divided into direct, relative and environment referred guidance. Though the first category is made of systems which are the most reliable, such as wire-guidance, etc., they are also systems which suffer from the considerable problem of path planning. If the path has to be changed, production must be stopped. The relative or dead-reckoning methods, such as encoders, gyroscopes, ultrasound, etc., have the considerable advantage of being totally self-contained inside the robot, relatively simple to use and able to guarantee a high data rate. On the other hand, since these systems integrate relative increments, errors grow considerably over time [17,18,19,20,21,22,23,24]. Environment referred guidance makes use of external references to achieve a measurement with respect to the environment where the robot is moving [3]. These systems are more complicated than the relative ones, work at a slower rate, and the current employed systems need visible artificial targets thus leading to the problem of the visibility of those targets during the robot’s path. However, since they measure the robot’s position and attitude with respect to references (targets), the error is always bounded and absolute repeatability guaranteed [3,19,20,21,22,23,24].

To achieve flexibility in path planning and robustness in accuracy, a combination of environment referred and

relative guidance [1, 2, 3] must be used by means of fusing the informations coming from sensors of the above categories. In this way it is guaranteed a high data rate and an error in pose estimation which is always bounded.

The most common industrial environment referred guidance system is the 2D laser scanner with reflective artificial targets. The main problems of this system are: it needs target visibility along the path, reflecting surfaces can be interpreted as reference targets, target are not directly distinguished one from another (matching methods must be embedded), high repeatability but low accuracy, switching from one layer of reflectors to another or simply masking some reflectors yields to pose discontinuities, external use is not recommended and the environment must be totally known [15].

For these reasons laser range sensors commonly used for safety and providing a 2D map of the surrounding environment are gaining an increasing interest. These sensors supplies about 5÷10 scans per second with an angle of 180° that can be used to localise the robot relating the pose to the features of the external environment whose map can be dynamically built [1, 7]. The development of accurate and robust guidance systems by means of these methods is therefore of great interest, in order to extend the use of autonomous robots to unknown or tough environments (such as outdoor applications or passages, long corridors, narrow passages, truck loading, only the starting and the target positions are known except the precise path, and other situations where static reflectors are not allowed or useful).

Some of the techniques used to estimate the robot pose from the laser scans relies on the extraction of natural landmarks and the application of Kalman filtering [1, 11], in particular [11] uses the lines extracted from the polygonal walls of the rooms in the update phase of the extended Kalman filter. In [8, 7] pose variation is computed from the histograms of the x and y co-ordinates and that of the range derivatives. In [10] pose is estimated by a recursive point to point assignment method. In [9] pose is estimated by a computationally efficient method optimised for polygonal rooms, by means of the matching of the rooms lines extracted from the scan data and Kalman filtering.

The above methods (except [9]) show a good performance in estimating narrow pose variations and therefore need an initial estimation of robot pose variation

coming from a different measurement system. In many cases the odometric or inertial estimation is available and accurate but there are other cases where these data are not available as in water robots or are inaccurate as for robots operating in harsh terrain. Furthermore the hypothesis of polygonal environment can be poorly matched in many environments.

For the above reasons we developed LS_NAV, a system that uses range data coming from safety rangefinders and which provides pose estimation with good accuracy performance both for large and short pose variations [16]. The input that must be provided to the system are the range in which the solution can be found and the timeout (maximum computation time allowed).

In order to optimise the computation load and have high data rate at disposal, we developed a custom sensor fusion technique that have the following characteristics: takes into account the correlation between the parameters uncertainty as a function of the calculation steps, propagates the relative system uncertainty taking into account the above correlations and the robot manoeuvres, fuses both wheel encoders output with the LS_NAV estimates also taking into account synchronization. This problem arises when fusing data corresponding to different time instants and those data are available with variable delays. Special care to this aspect was paid as explained in §4.

The algorithm proposed was implemented on an autonomous vehicle with differential kinematics. A PXI (National Instruments) with an embedded real-time operating system (RTOS) was used to control the robot and implement the navigation-fusion algorithm, a PC 104 with a different and independent RTOS was used to implement the LS_NAV system. This mock-up was used to estimate experimentally the accuracy of the LS_NAV system with the proposed sensor-fusion algorithm.

2. ODOMETRIC ESTIMATION

An odometric system using two encoders on the driving wheels were installed on the vehicle shown in Figure 1. The navigation equations of the differential drive and its uncertainty estimation are shortly explained in this section, deeper explanations can be found in [5] and [6].

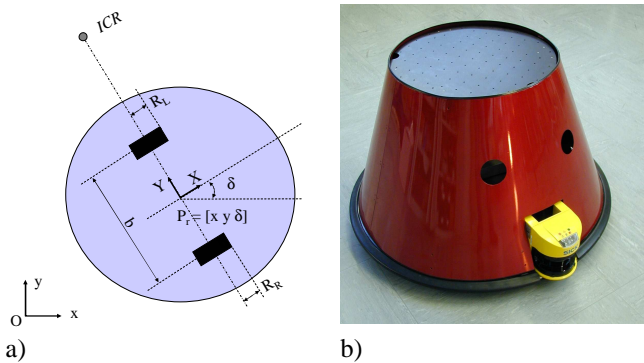


Fig. 1. a) Kinematics scheme of the differential drive AGV. The attitude d is the angle between the environment referred reference system xOy and the mobile reference system $XP.Y$. The pose P , is defined by the vector (x,y,d) which takes into account the attitude of the mobile robot. b) Photo of the autonomous vehicle.

The discrete form of the Odometric navigation equations is the following:

$$\begin{cases} x_{k+1} = x_k + \pi \cdot \frac{n_{Rk} \cdot R_R + n_{Lk} \cdot R_L}{n_0} \cdot \cos(\delta_k) \\ y_{k+1} = y_k + \pi \cdot \frac{n_{Rk} \cdot R_R + n_{Lk} \cdot R_L}{n_0} \cdot \sin(\delta_k) \\ \delta_{k+1} = \delta_k + 2\pi \cdot \frac{n_{Rk} \cdot R_R - n_{Lk} \cdot R_L}{b} \end{cases} \quad (1)$$

The definition of symbols relating to the equations shown in the paper can be found in the list of symbols at the end.

Uncertainty is expressed in terms of the covariance matrix of the vector $X_k^E = [x_k, y_k, \delta_k]$. In order to achieve the above covariance estimation, equation 1 can be rewritten as:

$$X_{k+1}^E = X_k^E + \Phi(w_k) \quad (2)$$

where Φ is a nonlinear function of $w_k = [n_{Rk}, n_{Lk}, R_R, R_L, b]$ that calculates the position increments at each iteration step. The standard uncertainty of the estimation X_{k+1} can be determined if the standard uncertainty of the estimates X_k and parameters w_k uncertainty C_{w_k} are known. The uncertainty can be expressed using the covariance matrix taking into account full correlation of the uncertainty parameters, like developed from the authors in [5, 6]:

$$C_{k+1}^E = C_k^E + \mathfrak{S}_{\Phi k} \cdot C_{w_k} \cdot \mathfrak{S}_{\Phi k}^T + \mathfrak{S}_{\Phi k} \cdot S_{w_k} \cdot I_k^T + I_k \cdot S_{w_k} \cdot \mathfrak{S}_{\Phi k}^T \quad (3)$$

where the integral term I_k can be evaluated using the following recursion:

$$I_k = I_{k-1} + \mathfrak{S}_{\Phi k-1} \cdot S_{w_{k-1}} \quad (4)$$

In the RT implementation the cycle time of the odometric estimation was $T_o = 15$ ms, therefore the time elapsed between two samples k and $k+1$ is 15 ms.

3. THE LS_NAV SYSTEM

The uncertainty of laser scanner measurements may influence the LS_NAV pose estimation.

In order to characterize the laser scanner measurements it has been mounted on a bar for optical alignment together with a panel hinged in the axis orthogonal to the bar, whose rotation is measured by means of an encoder with 14400 ppr, see Figure 2. By means of the above system it was first characterized the noise standard deviation that was estimated to be about 25 mm, then the effect of the following influence parameters on laser accuracy: temperature drift, distance, surface color, surface material and angle of incidence with respect to the object.

Above all influence quantities the angle of incidence plays a major role in degrading the measurement accuracy. This is due to the fact that this value may vary between the two scans. This situation doesn't happen for example for surface color which remains the same for the corresponding objects between the two scans.



Fig. 2. Experimental apparatus used for laser characterisation

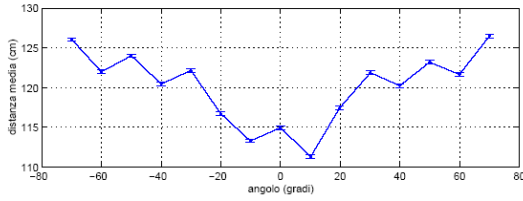


Fig. 3. Measurement as a function of the incidence angle. Measurements taken with the target at fixed distance of 155 cm with the apparatus of Figure 2.

The effect of the incidence angle over range estimation is shown in Figure 3. It comes out that differences of about 150 mm between the objects contour can arise only due to rotation or perspective effects.

The LS_NAV uncertainty of the pose variation estimate is expressed in term of a covariance matrix and it is also a function of the vehicle velocity (linear and angular). Therefore the overall estimate is expressed in the following way:

$$C_n^L = C_0 \cdot (1 + \alpha \cdot |v|^2) \cdot \left(1 + \beta \cdot \left| \dot{\delta} \right|^2 \right) \quad (5)$$

In the above formula the term C_0 is the covariance matrix estimated by the proprietary algorithm as a function of internal parameters and map matching verified during calibration. The system of units employed in the system described in §1 (see Figure 1) is the standard mks, the coefficient α and β are respectively 300 and 10^5 .

The method developed by us to estimate the relative displacement and attitude variation by means of the LS_NAV has not been explained in detail here because of industrial reserve.

4. DATA FUSION METHOD

The fusion between the odometric and the LS_NAV systems makes use of a method developed specifically for this purpose. Fusion between the two systems is in fact a non standard task because of the dependence of the LS_NAV measurement from an initial guess of pose and covariance (it is so to speed-up its calculation) and the time delay plus lack of synchronization between the two systems.

Like shown in Figure 4, the odometric pose and covariance estimation at time n is fed to the LS_NAV system that uses the pose like a reference point, the pose

variation to estimate the resulting uncertainty (equation 5), and the covariance to limit the field of possible solutions; synchronized data are fused by storing odometric estimate at sample n ; then the delay compensation between the time instant to which the fused estimate is referred and the time corresponding to the LS_NAV estimate and fusion, is computed. Furthermore, at a higher rate odometric pose and covariance are always recursively computed starting for its recursion from pose and covariance at sample n (to wait for the LS_NAV computation and compensate for its delay) or at sample $n+k$ (to wait for laser scan data to be collected).

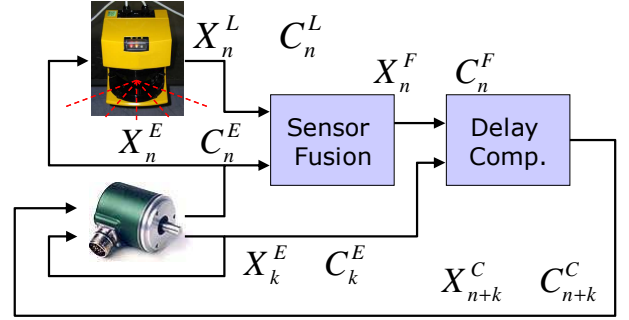


Fig. 4. Scheme of the recursive fusion algorithm.

The recursive fusion between the odometric and the LS_NAV estimation is combined taking into account the maximum likelihood criteria, therefore in the following way:

$$X_n^F = C_n^E (C_n^E + C_n^L)^{-1} X_n^L + C_n^L (C_n^E + C_n^L)^{-1} X_n^E \quad (6)$$

$$C_n^F = C_n^E (C_n^E + C_n^L)^{-1} C_n^L \quad (7)$$

The delay compensation is estimated by the following:

$$X_{n+k}^C = X_n^F + X_k^E \quad (8)$$

$$C_{n+k}^C = C_n^F + C_k^E \quad (9)$$

Equation 9 was obtained neglecting correlation between the fused estimate at time nT_l and the odometric estimate at time $nT_l + kT_o$; this was made possible by restarting the recursion of equations 2,3,4 at time nT_l and therefore considering only the increments in the elapsed time kT_o . This assumption simplifies dramatically equations 8 and 9 thus making the developed algorithm suitable for RT implementation.

In the RT implementation (onboard the PC 104 with CPU clock 200 MHz) the mean cycle time of the LS_NAV estimation was about $T_l = 500$ ms, while the scan data were available every about 143 ms.

Like already explained, during motion the computation time of about 500 ms must be taken into account in order to fuse the corresponding estimates (timely speaking) and compensating for its computation time.

Referring to Figure 5, the fusion method can be viewed from a procedural point of view:

1. the odometric pose estimate X_n^E and its covariance C_n^E at the time of laser scan data acquisition $T_s = nT_l$ are stored;
2. during the LS_NAV computation the odometric incremental pose X_k^E and incremental covariance C_k^E are computed;
3. the LS_NAV pose estimation X_n^L (that corresponds about to the same time T_s) and covariance C_n^L are computed;
4. fusion between the odometric and the LS_NAV estimates is computed: X_n, C_n ;
5. pose and corresponding covariance at time $T_s + kT_o$ are computed.
6. pose estimation is incremented by means of the odometric system until time $(n+m) \cdot T_l$ when the cycle restarts ($m \in \mathfrak{R}$ depends upon the current LS_NAV computation time).

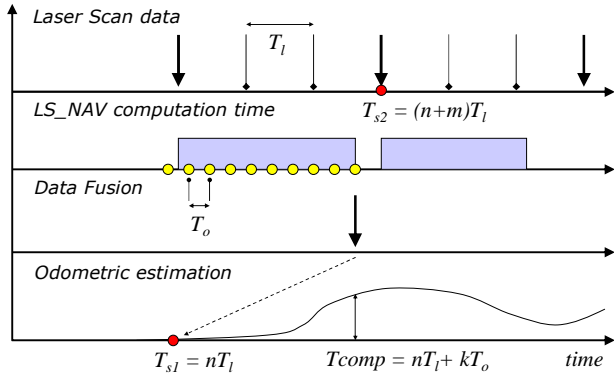


Fig. 5. Main events of the fusion algorithm as a function of time.

5. EXPERIMENTAL VERIFICATION

In order to verify the proposed technique experimentally, a mock-up of differential drive robot 1.1 m diameter (see Figure 1) was used. Two incremental encoders with 1000 ppr were mounted on the vehicle. An industrial safety laser rangefinder with a 40 m range and a 180° angular range with 0.5° angular resolution was mounted at the front of the vehicle and furnished the measured scans to the LS_NAV navigation algorithm.

The control references were generated for navigation and fusion recursion computed by an industrial PXI embedded system communicating with a PC 104 with a different and independent RTOS where the LS_NAV system was implemented.

In Figure 6 the acquired positions of a straight path plus a right-curve at about 30° are shown. The fusion algorithm was intentionally given a wrong initial position, 0.45 meters from the reference, so that if the only odometric system had been used it would have computed a completely wrong trajectory (see dashed black line in Figure 6). On the contrary, the fused pose, before the vehicle starts, converges in a few (five) iterations from the wrong initial pose to the

correct one because of the corrections computed by the LS_NAV system. The whole trajectory can be described as follows: at its first cycle the LS_NAV receives the wrong initial position (point “A”) and a large searching range (as a function of the large uncertainty of the initial pose) centered on that position; then its calculations converge to the reference pose (point “B”) thus leading the fused pose to converge too; at the end of the curve (point “C”) it is evident how far the pure odometric trajectory is from the fused, much more accurate, trajectory. The endpoint position was verified by means of a triangulation sensor [3] to be compatible with the LS_NAV endpoint estimation (i.e. inside its uncertainty ellipse), 22 mm distant from that.

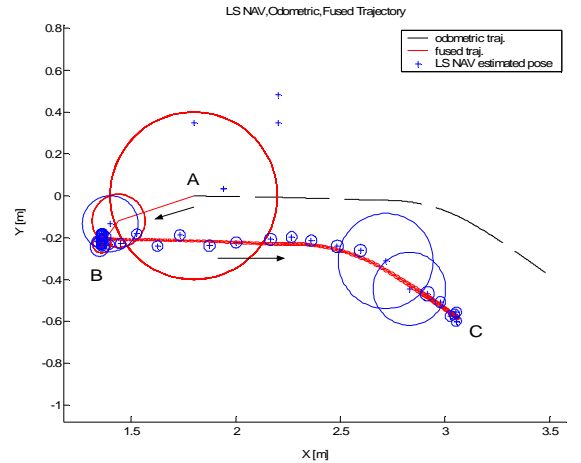


Fig. 6. Straight plus right-curve acquired path. The fused position, with large initial uncertainty, converges to the correct initial measure (from A to B), then its uncertainty diminishes

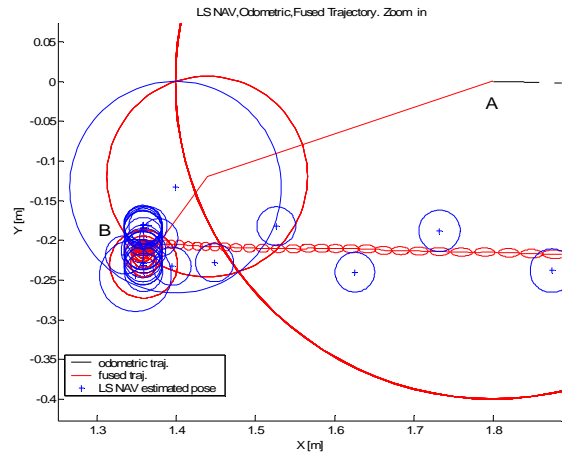


Fig. 7. Zoom on initial conditions of path. The LS_NAV pose estimate computed in a few steps on reference initial pose. Fused pose converges from the wrong initial pose assigned to odometric measurement system to the pose computed by the LS_NAV algorithm.

Figure 7 shows an enlargement of Figure 6 near the initial position. The red trajectory from point A to point B is not a movement of the robot but the convergence of fused pose from the wrong assigned initial pose to the correct one. Up to point B the vehicle is standing before moving toward point C.

In Figure 8 are shown (green squares) the searching ranges assigned to LS_NAV for each pose calculation. They

are computed as a function of the estimated covariance of fused pose which is assigned as an initial guess (i.e. the central point of the squares) to the LS_NAV algorithm.

In Figure 6,7,8 are also shown uncertainty ellipses of fused position and of LS_NAV position estimation.

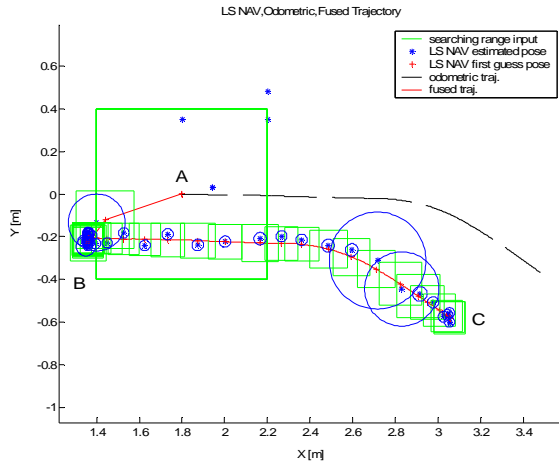


Fig. 8. In evidence initial guess of pose and searching fields of possible solutions derived from computed covariance given as an input to the LS_NAV algorithm.

Figure 9 and 10 show the acquisition of x-coord and attitude of fused and of LS_NAV pose of trajectory in Figure 6. The uncertainty bounds of fused x-coordinate are also shown.

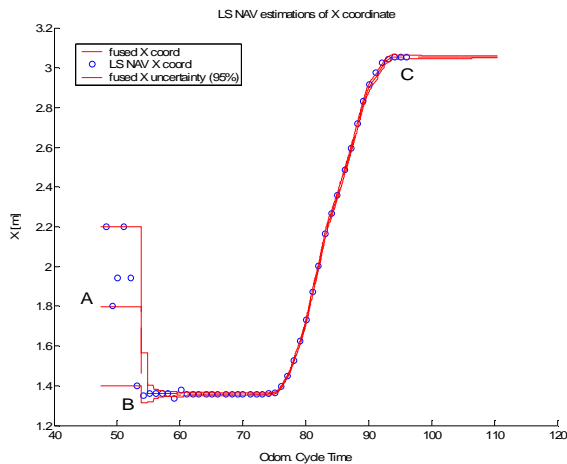


Fig. 9. Acquisition of x coord of fused pose and of LS_NAV pose of trajectory in Figure 6. Computed uncertainty bounds of fused x coordinate are showed.

In Figure 11 there is a zoom of Figure 10 where it is visible the increase of uncertainty during odometric trajectory estimation and the corresponding drop in uncertainty just after fusion (in Figure 5 shown as T_{comp}).

To verify the effectiveness of the developed system it was performed 25 closed loops. The fused trajectory is shown in blue and remains always close to itself (like what happened in reality), while the odometric pose estimation shows a remarkable drift.

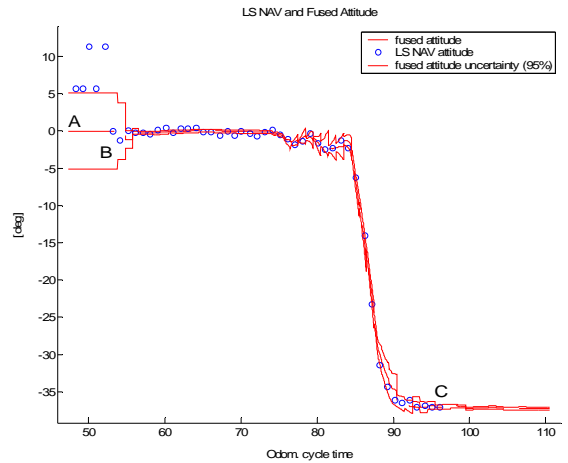


Fig. 10. Acquisition of attitude of fused pose and of LS_NAV pose of trajectory in Figure 6. Computed uncertainty limits of fused attitude are showed.

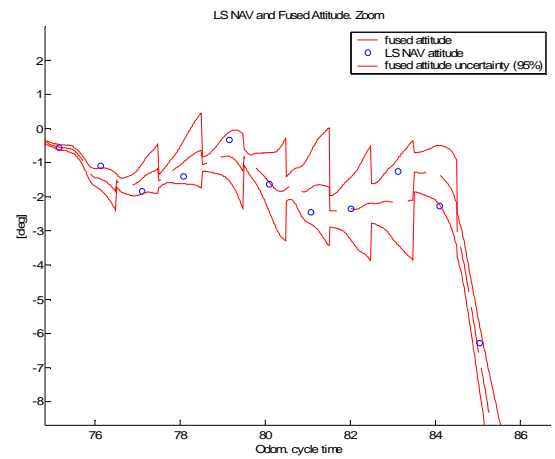


Fig. 11. Zoom in of attitude acquisition. Propagation of attitude uncertainty and its reduction after every fusion instant

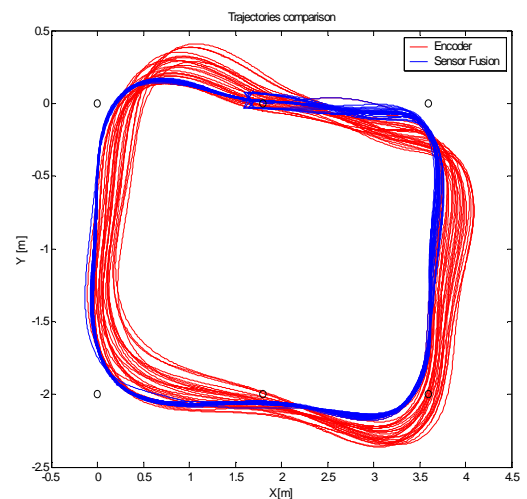


Fig. 12. Rectangular path, 25 turns. The odometric trajectory (in red) shows a drift for each turn while the fused trajectory with LS_NAV measurements (in blue) remains close to the reference path.

6. CONCLUSIONS

It is presented and discussed the data fusion application of the LS_NAV, a system that uses range data coming from safety rangefinders to provide pose estimation both for large and short pose variations in natural environment using random landmarks. Due to asynchronism (related to data communication) and computation time needed for pose estimation, it was developed a novel method for fusing odometric pose estimation with LS_NAV that takes into account both asynchronisms and time delays.

The method was tested on a real AGV. Details of the data fusion method are reported in §5 discussing the procedure and all the data involved.

The experimental test showed the ability of the system to converge to a solution also starting from a wrong initial estimate (about 0.4 meters far from the reference one) and the compatibility of its final pose estimation with a reference measurement system.

Finally, it was verified the effectiveness of the developed system by means of 25 closed loops that showed no drift or remarkable random behaviours.

LIST OF SYMBOLS

(x, y, δ)	the sensor fusion estimated position and attitude with respect to the fixed reference of the reference point P, on the vehicle
X_k	(x, y, δ) position and attitude vector at step k
C_V	covariance matrix of the vector V
R_R, R_L	the right and left driver wheels' radius
n_{Rk}, n_{Lk}	the number of counts from the driving right and left encoder
n_θ	the num. of counts of the driving encoder in one turn
b	the wheel base of the differential drive robot
$\mathcal{J}_{\Phi k}$	Jacobian matrix of the non linear function Φ_k
C_{wk}	diagonal matrix with covariances of parameters of w_k vector
S_{wk}	matrix whose elements are square root of C_{wk} elements

REFERENCES

- [1] E.M. Nebot, H. Durrant-Whyte. A High Integrity Navigation Architecture For Outdoor Autonomous Vehicles. *Robotics and Autonomous Systems*, Vol 26, p81-97, 1999.
- [2] J. Borenstein, H. R. Everett, L. Feng, D. Wehe. Mobile Robot Positioning - Sensors and Techniques. *Journal of Robotic Systems*, Special issue on Mobile Robots, vol. 14 n° 4, pp 231-249, 1997.
- [3] M. De Cecco. A new concept for triangulation measurement of AGV attitude and position. *Measurement Science and Technology*, vol 11, pp 105-110, 2000.
- [4] M. De Cecco. Self-Calibration of AGV Inertial-Odometric Navigation Using Absolute-Reference Measurements. *IEEE Instrumentation and Measurement Technology Conference*, Anchorage, AK, USA, 21-23 May 2002.
- [5] M De Cecco. Sensor fusion of inertial-odometric navigation as a function of the actual manoeuvres of autonomous guided vehicles. *Measurement Science and Technology*, vol. 14, pp 643-653, 2003.
- [6] De Cecco M., Baglivo L., Pertile M., Real-Time Uncertainty Estimation of Odometric Trajectory as a Function of the Actual Manoeuvres of Autonomous Guided Vehicles, *AMUEM 2006 - Sardinia*, Trento, Italy, 20-21 April 2006.
- [7] T. Rofer. Using Histogram Correlation to create consistent Laser Scan Maps. *IROS 2002*, EPFL, Lausanne, Switzerland pp 625-630, 2002.
- [8] G.Weiss, C.Wetzler, E.Puttkamer. Keeping Track of Position and Orientation of Moving Indoor Systems by Correlation of Range-Finder Scans. In *Proc. of the IEEE/RSJ International Conference on Intelligent Robots and Systems (IROS)*, 1994.
- [9] J.S.Gutmann, T.Weigel, B.Nebel. A Fast Accurate and Robust Method for Self-Localization in Polygonal Environments Using Laser-Range-Finders. *Advanced Robotics Journal*, 14(8), pp.651-668, 2001.
- [10] F.Lu, E.Milios. Robot Pose Estimation in Unknown Environments by Matching 2D Range Scans. In *Proc. of IEEE Conf. on Computer Vision and Pattern Recognition*, 1994.
- [11] P.Jensfelt, H.I.Christensen, Pose Tracking using Laser Scanning and Minimalistic Environmental Models. *IEEE Transactions on Robotics and Automation*, vol 17, no 2, April 2001.
- [12] G.Dissanayake, P.Newman, S.Clark, H.Durrant-Whyte, M.Csorba, A solution to the simultaneous localization and map building (SLAM) problem. *IEEE Transactions on Robotics and Automation*, Vol 17, No 3, p229-241, June 2001.
- [13] Cang Ye, J.Borenstein, Characterization of a 2-D Laser Scanner for Mobile Robot Obstacle Negotiation. *IEEE International Conference on Robotics and Automation*, 2002.
- [14] Luca Baglivo, Mariolino De Cecco, Francesco Angrilli, Francesco Tecchio, Angelo Pivato, An integrated hardware/software platform for both Simulation and Real-Time Autonomus Guided Vehicles Navigation, *ESM 2005*, Riga, Latvia, June 1st - 4th, 2005.
- [15] Internal Report, SMS-AITDIG-100-Caratt_SICK_NAV rev3, July 2005.
- [16] Internal Report, Pose Estimation in Unknown Environments by means of Laser Scanner Range Data: a Method for Large Displacements Estimation, December 2004.
- [17] B. Barshan, H.F. Durrant-White, Inertial Navigation Systems for Mobile Robots, *IEEE Transactions on Robotics and Automation*, Vol 11, No 3, June 1995.
- [18] J. Borenstein, L Feng, Measurement and Correction of Systematic Odometry Errors in Mobile Robots, *IEEE Transactions on Robotics and Automation*, Vol 12, No 5, Oct. 1996.
- [19] Adam, E Rivlin, H. Rotstein, Fusion of Fixation and Odometry for Vehicle Navigation, *IEEE Int. Conf. On Robotics and Automation*, Detroit, Michigan, May 1999.
- [20] S Shoval, I Zeitoun, E Lenz, Implementation of a Kalman filter in positioning for Autonomous Vehicles, and its Sensitivity to the Process Parameters, *Int J Adv Manuf Technol*, Vol 13, pp 738-746, 1997.
- [21] D. Bouvet, M. Froumentin, G. Garcia, A real-time localization system for compactors, *Automation in construction*, Vol 10, pp 417-428, 2001
- [22] S. I. Roumeliotis, G. S. Sukhatme, G. A. Bekey, Circumventing Dynamic Modeling: Evaluation of the error-state Kalman Filter applied to mobile robot localization, *Proc. 1999 IEEE International Conference on Robotics and Automation*, Detroit, May 10-15, pp. 1656-1663, 1999.
- [23] L. Jetto, S. Longhi, D. Vitali, Localization of a wheeled mobile robot by sensor data fusion based on a fuzzy logic adapted Kalman filter, *Control Engineering Practice*, vol 7, pp. 763-771, 1999.
- [24] Y. K. Tham, H. Wang, E. K. Teoh, Multi-sensor fusion for steerable four-wheeled industrial vehicles, *Control Engineering Practice*, vol. 7, pp. 1233-1248, 1999.
- [25] R. C. Smith, P. Cheeseman, On the representation and Estimation of Spatial Uncertainty, *int. J. Of Robotics Research*, Vol 5, no 4, pp 56-68, 1986.
- [26] Guide to Expression of Uncertainty in Measurements ISO 1993.